Judging the shape of moving objects: Discriminating dynamic angles

Graeme J. Kennedy
Department of Vision Sciences, Glasgow Caledonian University, Cowcaddens Road, Glasgow, UK

Harry S. Orbach
Department of Vision Sciences, Glasgow Caledonian University, Cowcaddens Road, Glasgow, UK

Gael E. Gordon
Department of Vision Sciences, Glasgow Caledonian University, Cowcaddens Road, Glasgow, UK

Gunter Loffler
Department of Vision Sciences, Glasgow Caledonian University, Cowcaddens Road, Glasgow, UK

Studies of shape perception have typically focused on static shapes. Studies of motion perception have mainly investigated speed and direction. None have addressed performance for judging the shape of moving objects. We investigated this by determining the discrimination of geometric angles under various dynamic conditions (translation, rotation, and expansion). Angles were parts of imaginary triangles, defined by three vertex dots. Compared to static angles, results show no significant decline in the precision of angle judgments for any of the three motion types, up to speeds high enough to impair target visibility. Additional experiments provide evidence against a uniform mechanism underlying static and dynamic performance, which could rely on "snapshots" when processing moving angles. Rather, we find support for distinct mechanisms. Firstly, adding noise dots to the display affects rotating and expanding angles substantially more than those which are translating or static. Secondly, the ability to judge angles is unaffected when vertex dots are occluded for short periods. Given the dependence of dot trajectories on the overall triangle motion, the ability to precisely extrapolate the future position of a dot requires distinct computations for translating, expanding, and rotating shapes.

Keywords: angle discrimination, shape perception, form perception, motion perception, optic flow

Citation: Kennedy, G. J., Orbach, H. S., Gordon, G. E., & Loffler, G. (2008). Judging the shape of moving objects: Discriminating dynamic angles. *Journal of Vision, 8*(13):9, 1–13, http://journalofvision.org/8/13/9/, doi:10.1167/8.13.9.

Introduction

Research on the perception of simple (Bouma & Andriessen, 1968; Orban, Vandenbussche, & Vogels, 1984; Scobey, 1982) and complex (Coppola, Purves, McCoy, & Purves, 1998; Elder & Goldberg, 2002; Farah, Wilson, Drain, & Tanaka, 1998; Field, Hayes, & Hess, 1993; Geisler, Perry, Super, & Gallogly, 2001; Valentine, 1991; Wilkinson, Wilson, & Habak, 1998) shapes has typically concentrated on static stimuli. Studies of motion perception have been concerned mainly with the discrimination of some aspect of the stimulus motion, e.g., direction (De Bruyn & Orban, 1988; Watamaniuk, Sekuler, & Williams, 1989) or speed (McKee, Silverman, & Nakayama, 1986; Nakayama, 1981; Stone & Thompson, 1992; Thompson, 1982), without focusing on the discrimination of the stimulus shape. Hence, on one hand are studies of shape perception that have largely ignored motion and, on the other, are studies of motion perception that have focused on the dynamics of the stimulus and paid little attention to its shape. Both approaches neglect complementary aspects of natural objects: they have a particular shape and are frequently moving. The accurate representation of both object shape *and* object motion is important when living in, and navigating through, a dynamic environment, and it is not clear whether data from studies of static shapes can be used to predict performance when shapes are in motion.

This leaves open the question as to how good we are at discriminating the shape of moving objects, especially in light of the fact that almost all movement produces some sort of shape deformation. The experiments described here aimed to address this question by investigating the discrimination of a simple shape, namely an angle, under dynamic conditions. Angle discrimination performance

doi: 10.1167/8.13.9 Received January 17, 2008; published October 29, 2008 ISSN 1534-7362

was measured for various motion types and speeds, and performance under these conditions was compared with that for static stimuli.

Methods

Stimuli

In all experiments, the angle to be judged ("apex angle") was part of an imaginary triangle that was defined by a "dot" at each vertex (see Figure 1). Discrete dots force the visual system to combine information across space and extrapolate the shape of the triangle. We selected the spatial frequency of the dots, and the distance between them, such that no two dots would fall within the same receptive field of a neuron in the primary cortical visual area (V1).

The contrast cross-section profile of each corner dot was given by a circularly symmetric fourth derivative of a Gaussian (D4):

$$\mathrm{D4}(r) = c \cdot \left(1 - 4\left(\frac{r}{\sigma}\right)^2 + \frac{4}{3}\left(\frac{r}{\sigma}\right)^4\right) \cdot e^{-\left(\frac{r}{\sigma}\right)^2} \qquad (1)$$

In Equation 1, D4(r) describes the normalised luminance value at each pixel in a polar coordinate system, r is the radius in degrees of visual angle with respect to the center of the location of the dot, σ (in degrees of visual angle) determines its peak spatial frequency, and c denotes contrast. In all experiments, the mean distance between the center of the apex dot and each peripheral dot ("l_1" and "l_2") subtended 1.75 degrees. The distance between dots was fixed for each stimulus presentation but was varied randomly and independently (by up to ±30% of the mean distance) between presentations. The lengths of l_1 and l_2 were defined by the following equations:

$$\begin{aligned} l_1 &= l_{\mathrm{mean}} + [(2 \cdot \mathrm{rand} - 1) \cdot 0.3 \cdot l_{\mathrm{mean}}] \\ l_2 &= l_{\mathrm{mean}} + [(2 \cdot \mathrm{rand} - 1) \cdot 0.3 \cdot l_{\mathrm{mean}}] \end{aligned} \qquad (2)$$

In Equation 2, l_{mean} is the average distance and "rand" is a random number from a uniform distribution [0–1]. This randomization prevents observers using the length of the invisible side of the triangle opposite the apex angle (i.e., distance between the two peripheral dots) as a cue to angular magnitude (Regan, Gray, & Hamstra, 1996).

It is also possible that observers may base their judgment of an angle on a change in the absolute orientation of one or both of the sides of the triangle (Regan et al., 1996), even when these sides, as in our experiments, were not made explicit. While this is unlikely in the case of rotating triangles, it is an important consideration for expansion and translation and in conditions where stimuli are static. Therefore, the initial orientation of each triangle, defined as the orientation of the triangle's apex angle bisector, was chosen randomly (within 0°–360°) for each presentation.

Stimulus motion

Theoretical and empirical evidence supports the view that different types of motion (rotation, translation, and expansion/contraction) are processed differently (Albright, 1984; Burr, Morrone, & Vaina, 1998; Duffy & Wurtz, 1991; Koenderink, 1986; Morrone, Burr, & Vaina, 1995; Movshon & Newsome, 1996; Tanaka & Saito, 1989). A full investigation of the perception of shapes in motion should, therefore, include all of these motions. As such, the experimental stimuli comprised movie sequences

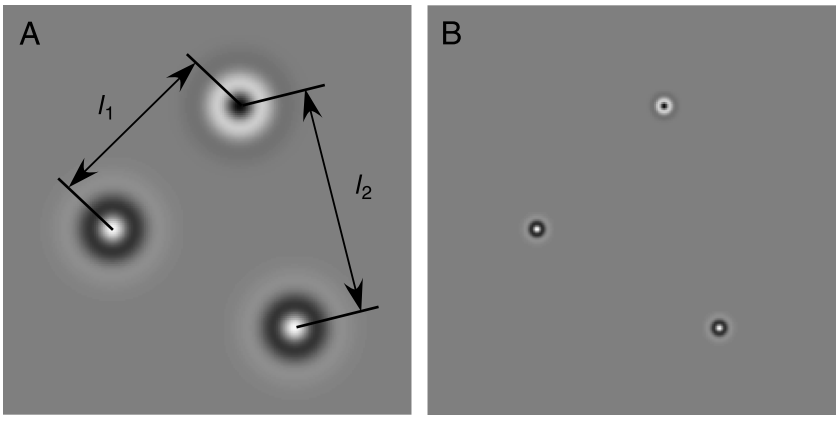

Figure 1. Stimuli. The angles to be compared were parts of imaginary triangles, which were defined by a "dot" at each vertex. Each dot profile was that of a D4 with a full spatial frequency bandwidth of 1.24 octaves at half amplitude. Two different dot spatial frequencies were used; 2 c·deg^{-1} (A) and 8 c·deg^{-1} (B). Different contrast polarities were used to mark the location of the angle to be judged: the contrast of the dot at the location of the apex angle was set to −98% (the top angle in these figures) and the remaining two dots to +98%. "l_1" and "l_2" are the lengths of the sides of the triangle which enclose the angle.

showing triangles rotating, translating or expanding rigidly in the fronto-parallel plane (Figure 2). In the conditions where the stimuli were stationary, a single frame from a movie sequence was selected and was displayed for the entire stimulus interval.

It is worth noting that the nature and relationship of the trajectories of the three vertex dots depends on the type of motion. For translation, the situation is the simplest as all trajectories are linear and the speed and direction of each dot is identical. Expansion is more complex as, although trajectories are still linear, they generally differ in direction and speed. Rotation is the most complex. Trajectories are no longer linear, but arcs of circles. Consequently, trajectories not only differ in speed and direction but the direction of each dot changes over time. As will be discussed later, these stimulus differences have consequences for shape perception in some circumstances.

Observers

Three of the authors, all of whom were experienced in psychophysical tasks, participated in these experiments. All three observers had normal or corrected-to-normal vision (visual acuity of 6/6 or better).

Procedure

The screen background was initially set to mid-gray. A fixation dot appeared on the center of the screen at the beginning of each trial and disappeared, for the duration of the presentation, immediately before stimulus presentation. Subjects were encouraged to maintain fixation. The method of constant stimuli was employed in a temporal two-alternative forced choice paradigm. Each trial was initiated by pressing a key on the keyboard. This was followed by two temporally separated stimulus intervals. In each interval a movie sequence of a triangle moving with a particular type of motion at a particular speed, or in baseline conditions a static triangle, was displayed. Different conditions were run in separate experiments. The time between pressing a key and the onset of the first stimulus interval was 300 ms.

Angle discrimination performance was measured for six different angular magnitudes, distributed symmetrically around a reference angle. The values of these increments, relative to the reference angle, ranged from [±5°, ±10°, ±15°] to [±10°, ±20°, ±40°] depending on observer sensitivity and test condition and were determined in pilot runs. One of the stimulus intervals always contained the reference angle and the other contained one of the six increments. The order of stimulus presentations within each trial (i.e., reference angle in the first or second interval) was chosen randomly. Note that reference and test stimuli always showed the same type of motion and moved at the same speed. At the end of each trial, the observer pressed one of two keys to indicate which interval had shown the triangle with the more obtuse apex angle. Each increment was presented 30 times, giving a total of 180 trials per experiment. The resulting data were fitted by a Quick (1974) function using a maximum likelihood procedure. Angle discrimination thresholds were defined as half the distance between the 25% and 75% correct points on the resulting psychometric function. For each condition, each observer carried out at least two experimental runs, usually on different days, and separate threshold estimates were averaged.

Apparatus

Stimuli were presented on a LaCie "electron22blue" high-resolution monitor controlled by an Apple Power-Mac G4 computer. The frame refresh rate of the monitor was set to 85 Hz and the spatial resolution to 1024 × 768 pixels. Stimuli were displayed on a central portion of the monitor screen subtending 6.52 deg × 6.52 deg. Display calibration was achieved by measuring the luminance of each of the 256 monitor gray levels with a photometer (Minolta LS110) and then selecting a subset (151) of these that maximized contrast linearity with approximately equal incremental steps. Pattern luminance was modulated about a mean of 61 $cd \cdot m^{-2}$. Subjects viewed the stimuli binocularly under dim room illumination and a chin and forehead rest was used to maintain a constant viewing distance of 120 cm. At this distance, each pixel subtended 0.0177 deg. To avoid reference cues, the monitor frame was covered with a white cardboard mask with a circular aperture subtending 9 deg in diameter. Movies were calculated in MATLAB prior to the experiments. The patterns were displayed using custom-written Pascal code within the CodeWarrior environment.

Results

Unless otherwise stated, stimulus parameters were as follows: speeds were 180 $deg \cdot s^{-1}$ for rotation (i.e., the triangle underwent half of a full rotation per second) and 3.7 $deg \cdot s^{-1}$ for translation and expansion, reference angles were 60° and peak spatial frequency of the dots was 8 $c \cdot deg^{-1}$.

Discrimination of angles in motion

In the first experiment, the effect of different motion types (rotation, translation, and expansion) on the precision of angle discrimination was measured and compared with the static case (Figure 3). Discrimination thresholds across the dynamic and static conditions are not significantly different. Observers are able to discriminate angles

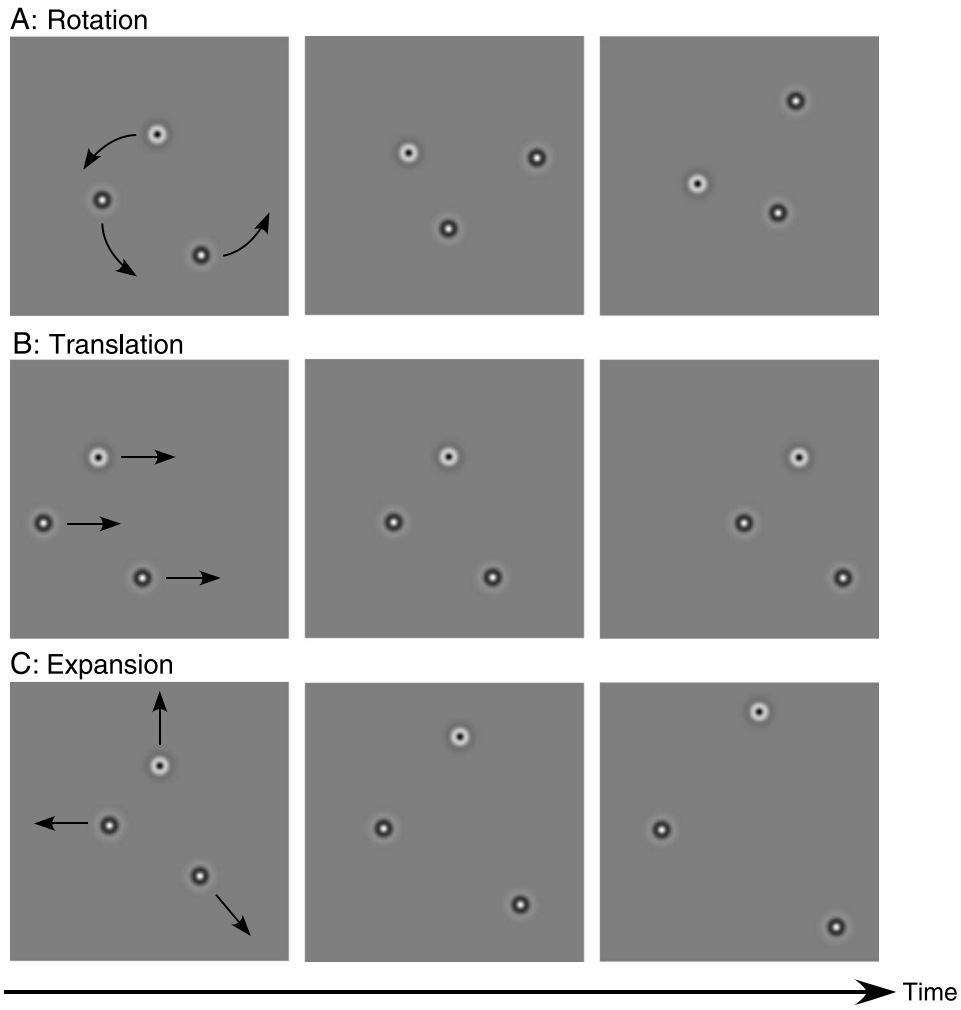

Figure 2. Different motion types used in the experiments. The stimuli were movie sequences of triangles defined by three dots. Each movie consisted of 34 frames and successive frames were presented in synchrony with the monitor refresh rate (Pelli, 1997). For a frame refresh rate of 85 Hz, this resulted in movies of 400 ms duration. Three types of motion were used: rotation (A), translation (B), and expansion (C). Three frames of an example movie sequence are shown for each type of motion. The movie sequences were created in a distinct way for each type of motion. (A) In the case of rotation, the location of the center of rotation had to be set. This was placed close to the apex dot. This position was chosen to avoid the inadvertent cues to the magnitude of the angle available when, for example, the center of rotation is placed at the triangle's circumcenter (as the apex angle increases, the dots move at increasingly faster speeds allowing the observer to discriminate angles by comparing the speeds of the stimulus dots) or at the triangle's centroid (as the angle increases, the centroid moves closer to the apex dot, which in turn moves more slowly if the overall rotational speed of the triangle is kept constant). To add a small amount of spatial uncertainty and avoid a static apex dot, the center of rotation for the triangle was chosen randomly from within a square region, centered on the apex dot, with side length 1 deg. Triangles were rotated randomly clockwise or counterclockwise at various speeds, defined in degrees of rotation per second, where 360 deg·s^{-1} represents a full triangle rotation per second. (B) For translational motion, the triangle was initially placed on one side of the monitor screen and then translated randomly either to the right or left. Given that performance may be speed dependent, every effort was made to match as closely as possible the speed of the stimulus dots across different motions, so that performance for different motion types could be compared. One way of doing this is to match the speed for translating triangles to the mean linear speed of the 3 dots in the rotating case. When the center of rotation is, on average, located at the center of the apex dot and the mean lengths of the two sides defining the angle (l_1 and l_2) are 1.75 deg, the apex dot moves at a speed of 0 deg·s^{-1} and the other two (peripheral) dots at mean speeds of [1.75 $\times$ π/180 $\times$ rotational speed]. To match a rotational speed of 180 deg·s^{-1}, for example, we used the equivalent average linear speed of the three dots (3.7 deg·s^{-1}) for translating triangles. Note that the specific algorithm used to calculate equivalent speeds is, in fact, not important: sensitivity is similar across a wide range of speeds (Figure 4A). (C) For triangles with expanding motions, each triangle's centroid was placed at the center of the screen. This point also acted as the center of expansion. The absolute linear speed of the apex dot in the case of expansion matched that of translating triangles. In order to retain shape constancy, the speed of the other two vertex dots depended on their distance from the center of expansion relative to the apex dot. In order to retain a constant rate of expansion, the speed of each dot was constant throughout the presentation. Direction of motion (outward versus inward) was varied randomly, resulting in expanding or contracting triangles.

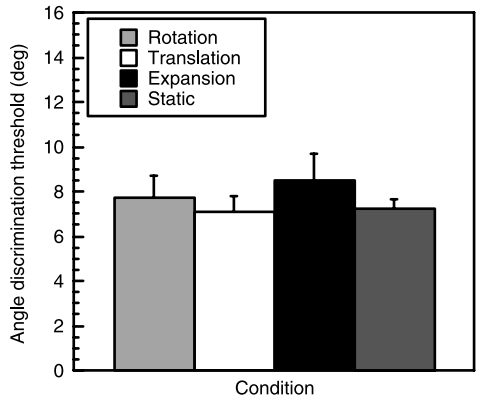

Figure 3. Angle discrimination for moving and static triangles. Thresholds are shown for three different types of motion, along with a static condition for comparison. Data are the means for three observers and error bars, here and elsewhere, show standard errors of the mean. Statistical analysis by means of an ANOVA confirms that there is no significant difference between different conditions ($F_{3,8}$ = 0.53, p = 0.68): angle discrimination is the same whether triangles are static or moving (rotating at 180 deg·s^{-1}, translating or expanding at 3.7 deg·s^{-1}).

to an accuracy of 7°–8°, whether they are static or moving, regardless of the type of motion. Although precision for discriminating static angles can be substantially higher when angles are defined by bounding lines (Chen & Levi, 1996; Heeley & Buchanan-Smith, 1996; Kennedy, Orbach, & Loffler, 2006; Regan et al., 1996), the level of sensitivity measured here is consistent with previous static investigations of angles defined by vertex dots, which showed thresholds to be in the range of 2.5°–13° (Heeley & Buchanan-Smith, 1996; Kennedy et al., 2006; Snippe & Koenderink, 1994). Adding motion does not affect performance when judging an angle embedded in a triangle, at least at the speeds tested here.

Effect of rotational speed

We next assessed if angle discrimination was affected by speed. To minimize the effect of smooth pursuit eye-movements triggered by translation and to keep the stimuli at a constant eccentricity, independent of speed, only rotation was considered here. Constant eccentricity is important since angle discrimination for static stimuli has been shown to depend on stimulus size (Werkhoven & Koenderink, 1993) and on stimulus eccentricity (Chen & Levi, 1997; Werkhoven & Koenderink, 1993).

Angle discrimination thresholds were determined for rotational speeds between 0 and 900 deg·s^{-1} (2.5 rotations per second). Performance depends on rotational speed and thresholds increase with increasing speed. Performance deteriorates noticeably only for very fast rotational speeds of more than 480 deg·s^{-1} (Figure 4A). Higher speeds (≥600 deg·s^{-1}) are required for performance to decrease

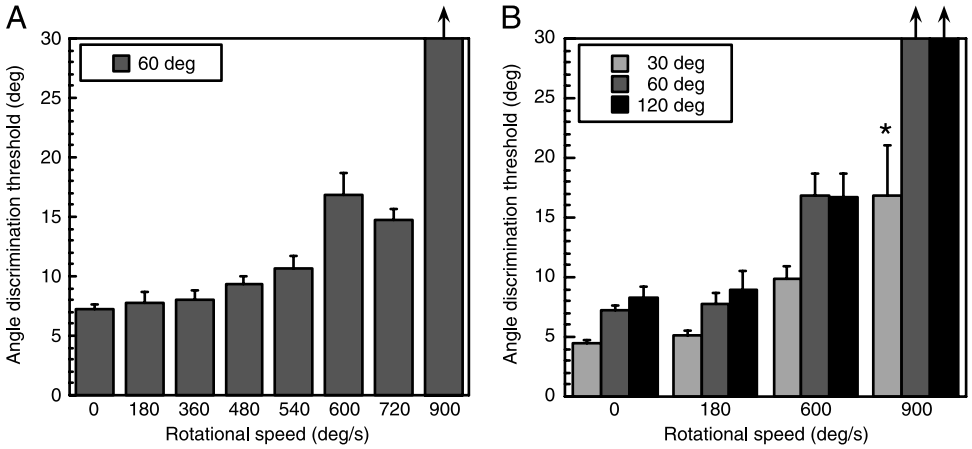

Figure 4. Effect of speed and reference angle on discrimination of rotating angles. (A) Mean angle discrimination thresholds for three observers are shown as a function of rotational speed. Thresholds are independent of speed, up to speeds of 480 deg·s^{-1}. Compared to the static (0 deg·s^{-1}) condition, ANOVA post hoc tests (Fisher's PLSD, at 5% significance level) show no cost to performance (p = 0.72, p = 0.54 and p = 0.13) for 180, 360, and 480 deg·s^{-1}, respectively. Even for a speed of 540 deg·s^{-1}, there is only a slight (but significant) increase in thresholds (p = 0.02). Faster speeds cause a noticeable decrease in performance. For a speed of 900 deg·s^{-1}, thresholds are outside the measurable range (>40°, as indicated by the vertical arrow on the rightmost column). (B) Angle discrimination thresholds were measured for three different reference angles, for triangles rotating at various speeds. The same pattern of results is seen for each reference angle. Average performance is the same whether angles are static or moving at a speed of 180 deg·s^{-1} (p = 0.69), but thresholds increase for speeds of 600 deg·s^{-1} or more (p < 0.0001). Additionally, thresholds are lower for a reference angle of 30° compared to larger angles of 60° and 120° (p < 0.001) but no difference is seen between the two larger angles (p = 0.69). Superior discrimination performance for smaller angles is in agreement with some studies of static angle discrimination, which have shown thresholds to increase with reference angle (Chen & Levi, 1996; Heeley & Buchanan-Smith, 1996, cf. Regan et al., 1996). The asterisk and the vertical arrows indicate that thresholds were above the measurable limit for one or all three observers, respectively.

markedly. At the highest speed (900 deg·s^{-1}), observers' performance was below 75% correct even for the largest stimulus increments tested (±40°), making it impossible to quantify thresholds. This general pattern of results is also seen for more acute (30°) and more obtuse (120°) reference angles and is therefore independent of the reference angle (Figure 4B).

Effect of stimulus spatial frequency

Previous psychophysical experiments using contrast-reversing gratings have shown that as temporal frequency is increased, contrast sensitivity for high spatial frequencies reduces whereas sensitivity for low spatial frequencies shows an increase (Kelly, 1979; Robson, 1966). It is conceivable, therefore, that the decrease in performance for high rotational speeds is due to reduced visibility rather than speed *per se*. If this were the case, decreasing the stimulus spatial frequency may improve performance at high speeds. In order to investigate this possibility, angle discrimination was next measured for a reduced dot spatial frequency of 2 c·deg^{-1} at rotational speeds of 0, 180, 600, 720, and 900 deg·s^{-1}.

Angle discrimination thresholds for the two spatial frequencies (2 and 8 c·deg^{-1}) are shown in Figure 5 as a function of rotational speed. For static stimuli and for speeds up to at least 180 deg·s^{-1}, performance is independent of dot spatial frequency as well as speed. Importantly, for higher rotational speeds (≥600 deg·s^{-1}), performance is better for the lower spatial frequency. Using the definition that the speed of a grating is equivalent to its temporal frequency divided by its spatial frequency, we can calculate equivalent temporal frequencies for the D4 stimuli in our experiments. This calculation yields temporal frequencies well outside the window of visibility for the higher frequency dots and values close to the limit for the lower frequency dots. This suggests that the reduction in discrimination performance seen at high rotational speeds is, at least to some extent, due to a reduction in dot visibility. We are therefore left with the striking result that the precision of angle judgments is high even when the stimulus dots are moving at a speed that puts them close to their spatio-temporal limit of visibility.

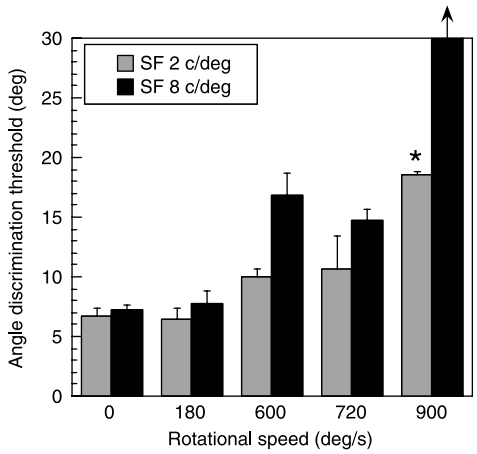

Figure 5. Effect of dot spatial frequency on discrimination of rotating angles. Mean angle discrimination thresholds are shown for three observers for spatial frequencies of 2 c·deg^{-1} (light bars) and 8 c·deg^{-1} (dark bars) at various rotational speeds. Up to a rotational speed of 180 deg·s^{-1}, performance is independent of spatial frequency and speed. For higher speeds, thresholds are lower (performance better) for the lower spatial frequency. For the highest speed (900 deg·s^{-1}), thresholds were outside the measurable range for all subjects when the spatial frequency of the dots was 8 c·deg^{-1} (arrow). In contrast, for the low frequency at the same speed, thresholds could be obtained from two of the three observers. The corresponding column is the mean of two observers only, indicated by an asterisk. Given that observers did not reach thresholds for increments of ±40° for a spatial frequency of 8 c·deg^{-1} and speed of 900 deg·s^{-1}, the mean discrimination performance (about 20°) for the same speed but lower frequency indicates that sensitivity is at least twice as high for the lower than for the higher frequency.

Computational strategies for dynamic angle discrimination

The experiments so far have shown that angles can be discriminated equally well whether they are static or moving, independent of the type of motion and up to high speeds. The most obvious and parsimonious candidate to account for this is a single mechanism that responds equally well to static and moving angles. Assume that the visual system has access to the location of each of the three dots of a triangle, say via activation within a retinotopic map (e.g., V1), and bases its computation of angular magnitude on the trigonometric relationship between these dots (see Figure 8A). If activation could be triggered by static as well as animated dots, as would be the case for simple cells in V1, and a computation based on "reading" this map, then there would be the same performance for static and dynamic angles. This computation essentially takes a "snapshot" from each movie sequence, thereby making the motion irrelevant and turning a seemingly dynamic task into a static one.

One way to investigate this possibility is to superimpose the moving angle on a background of static "noise" dots that are identical to those defining the triangle (Figure 6A). If using snapshots was the only strategy available to the visual system, then adding static dots to the display should impair performance for moving angles, as, in any single frame, the "triangle" dots are indistinguishable from the background. We extended this paradigm and considered, in addition to static background dots, the situation where the background dots were animated (Figure 6B). Choosing

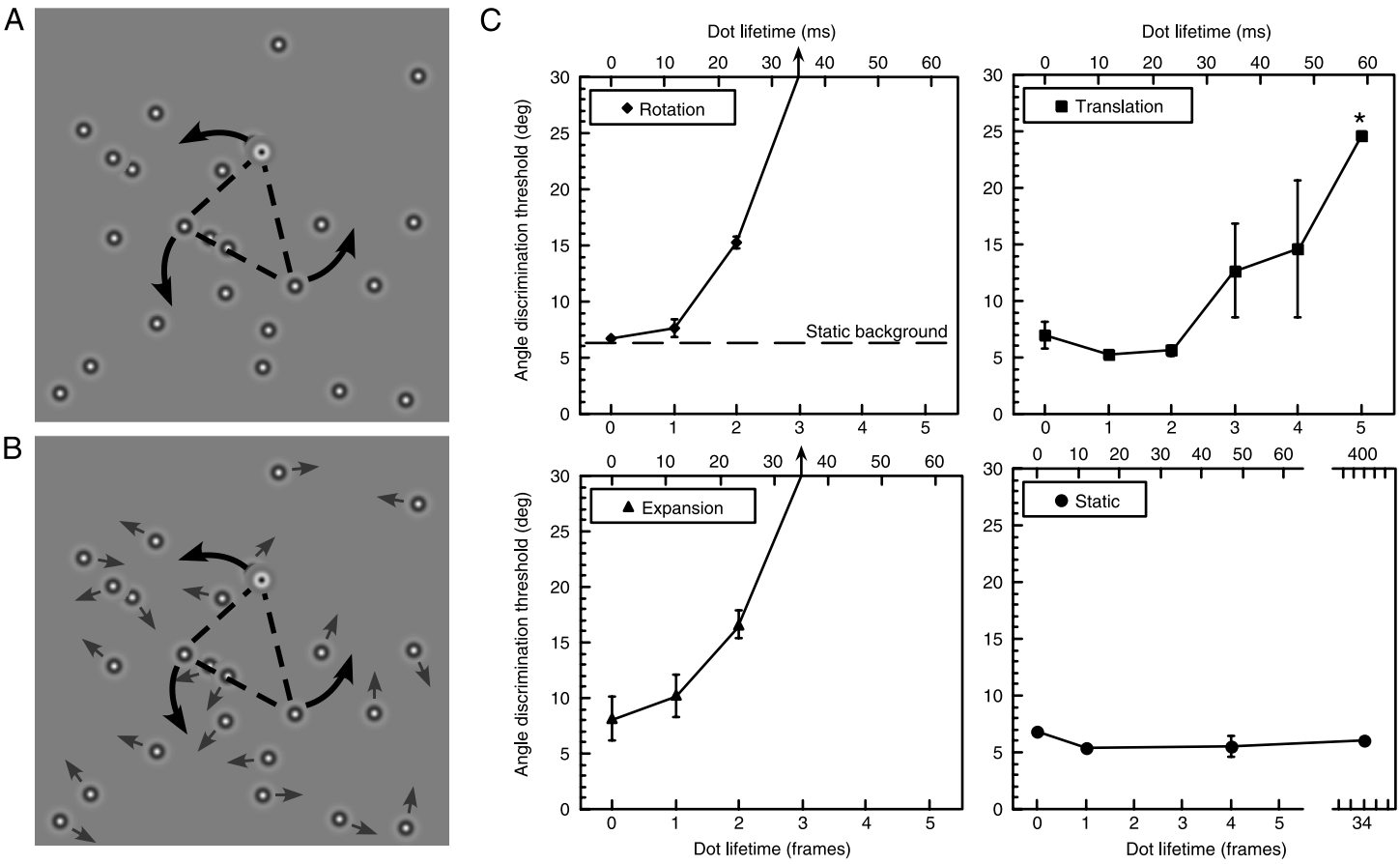

Figure 6. Adding background "noise" dots to the display. Movies of rotating, translating, or expanding triangles were superimposed on a pattern of background dots. "A" shows an example of a rotating triangle on a background of static dots and "B" an example of a rotating triangle with animated background dots, where each background dot moved along a linear trajectory in a random direction. For the sake of clarity, the arrows depicting the motion of the stimulus triangle are larger and darker than those depicting the motion of the background. This is not, however, an indicator of their relative speeds. The speed of the background dots was chosen to match that of the stimulus dots. Background dots were replaced after a certain number of frames (the "dot lifetime"). For example, if the dot lifetime was two, then after every second frame of the movie a new random background dot pattern was generated and displayed (actually half of the background dots were replaced in even-numbered frames and the other half in odd-numbered frames). Here, a dot lifetime of zero represents the situation where no background dots are present. The background dots were identical (contrast = +98%; SF = 8 c·deg^{-1}) to two of the triangle's vertex dots and were presented with a density of 20%. (C) Angle discrimination for static, rotating, translating, and expanding triangles in the presence of background dots. Thresholds are the mean for two observers. Performance for a triangle rotating on a background of static dots (dashed line in the upper left plot) is the same as when no dots are present (p = 0.55). All other data are for triangles presented on a background of animated dots, as a function of the lifetime of the background dots. For all types of moving triangles, thresholds increase with dot lifetime but at different rates. For rotation and expansion, performance reduces at a lifetime of 2 frames and, at 3 frames, thresholds are above the measurable limit (indicated by arrows). In the case of translating motion, thresholds do not increase for lifetimes of less than 3 frames. The asterisk for a 5-frame lifetime indicates, as before, that thresholds were only obtained for one observer and were outside the measurable range for the other. In contrast to the moving stimuli, performance for static triangles on a background of moving dots remains unaffected even when the background dot lifetime extends over the entire length of the movie (34 frames). Note that for a monitor refresh rate of 85 Hz, one frame lasts for 11.76 ms. Note also that the movie icon accompanying this article clearly demonstrates that as the background dot pattern changes (from no background dots to static dots to animated dots with an increasing lifetime) the visibility of the rotating target triangle becomes increasingly impaired.

the lifetime of the background dots as the independent parameter enables us to determine the length of the period over which information is integrated in the case of dynamic angles. Under the assumption that the relevant mechanism integrates information over a period of n frames, such a mechanism will not be able to distinguish the stimulus dots from the animated background dots if the background dots have a lifetime of n frames or more.

The general trend of the results (Figure 6C) for moving triangles is that, as the background dot lifetime increases, angle discrimination thresholds increase. Interestingly, performance decreases at different rates for different types

of motion. Rotation and expansion are more fragile than translation. For rotation and expansion, performance already deteriorates at a lifetime of 2 frames (23.5 ms) and a lifetime of 3 frames (35.3 ms) renders the task impossible. For translation, thresholds are unaffected by lifetimes of less than 3 frames but decrease for longer dot lifetimes. In contrast to the dynamic cases, performance for static triangles with moving background dots does not show a dependence on lifetime but remains equally good even when the lifetime of the background dots extends over the entire movie (34 frames = 400 ms).

One would expect the time courses for the different conditions to be the same if the same mechanism encoded dynamic and static angles. Our data do not support this hypothesis. In contrast to static angles, where adding static background dots (without replacing them) renders the task impossible (since it is impossible to determine which three dots form the triangle), adding static background dots to dynamic triangles (e.g., in the case of rotation: dashed line in upper left plot of Figure 6C) does not affect performance. This argues against the proposition that thresholds in dynamic and static conditions are determined by the same mechanism that relies on positional information arising from the same detectors (e.g., simple cells). Rather, the data support the existence of distinct mechanisms for static angles on one hand and dynamic angles on the other. Moreover, the finding that performance shows a different dependence on noise lifetime for rotation and expansion versus translation suggests that different mechanisms underlie different motion patterns.

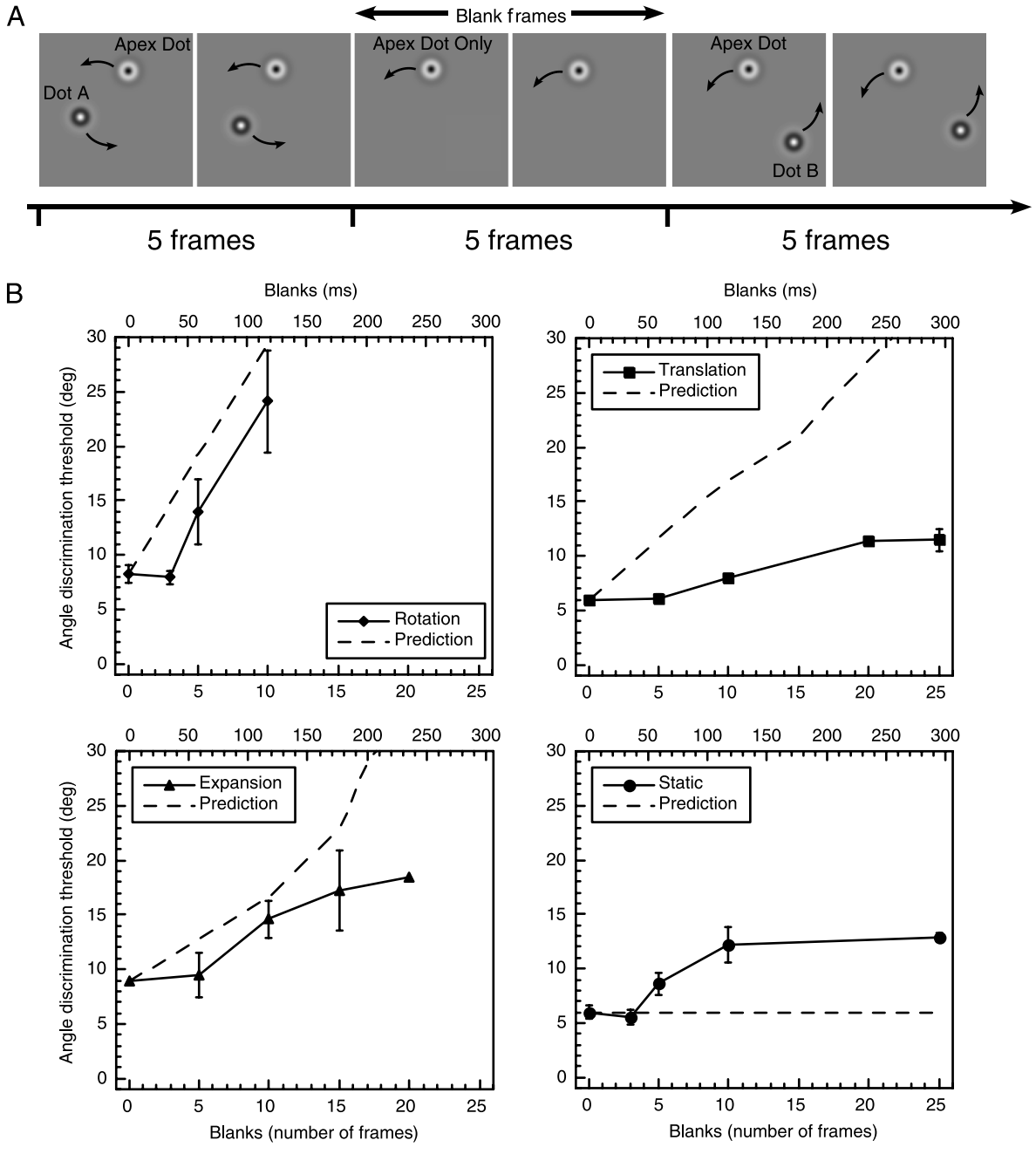

One obvious advantage of using different mechanisms to process dynamic angles, depending on the specific type of motion, is that specific mechanisms can be more resistant against the influence of factors such as noise or occlusion than a uniform computation. To investigate this further, we measured how accurately the visual system can extrapolate the location of a dot during a period of occlusion. This was done by manipulating individual dots so that, in particular frames, dots could be visible or not, as if they were switched on and off or disappeared (and reappeared) behind invisible occluders (Figure 7A). In every frame, one or the other of the vertex dots was invisible. Angle discrimination thresholds show a dependence on the duration of occlusion ("blank period," Figure 7B). The first significant result to note is that regardless of the type of motion, there is a short blank period of 3 (for static and rotation) to 5 frames (translation and expansion), where performance remains the same as for no blank period. Once the blank period exceeds these durations, angle discrimination thresholds increase with blank duration. The rate at which thresholds increase as a function of blank period depends on the type of motion. In the case of translation, there is only a relatively small effect on performance even for a very long blank period of 25 frames (295 ms); performance drops only by a factor of approximately 2 over this range. This is similar for static triangles. However, for expansion, performance deteriorates more quickly and, for rotation, there is the strongest effect of occlusion duration, with performance reducing noticeably when the two dots are separated by a blank period of only 5 frames (59 ms).

In summary, the discrimination of static versus dynamic angles shows different behavior under certain conditions (adding noise and introducing occlusion), suggesting that different mechanisms process angles depending on their dynamics.

Figure 7. Effect of dot "occlusion." (A) At the beginning of the movie, only the apex dot and one of the other vertex dots (e.g., peripheral dot "A") were present. After a certain number of frames, peripheral dot "A" disappeared. A variable "blank period" was introduced, in which only the apex dot was displayed. Following this blank period, the other vertex dot (e.g., peripheral dot "B") appeared at the location where it would have been, had it been present, and moving, all the time from the beginning of the movie (i.e., as if it had been occluded until now). This cycle was repeated until the end of the movie sequence so that the three dots were never simultaneously present. Each of the peripheral vertex dots was present for 5 frames (59 ms) before being occluded and the blank period varied from 0 to 25 frames (294 ms). (B) Performance for rotation (top left), translation (top right), expansion (bottom left), as well as for static stimuli (bottom right), is shown as a function of blank period. Data are the mean for two observers. Angle discrimination depends on the duration of the blank period. Performance is unaffected by short blanks (between 3 and 5 frames depending on the condition) but deteriorates for longer blanks. The rate at which blanks affect performance depends on the motion type: static and translating triangles show the weakest, expansion intermediate, and rotation the strongest dependence. To compare this performance with what would occur if the visual system did not extrapolate dot position, we calculated angular magnitudes of triangles defined by the apex dot and the position of one of the peripheral dots just before it disappeared and the position of the other dot when it appeared. This produces systematic biases of judgment, which depend on a number of parameters including speed and type of motion, triangle size, triangle orientation (for translation), the order of dot appearance (i.e., which dot is visible before and which after the blank), and the direction of motion (e.g., expansion versus contraction). Biases can result in angles larger as well as smaller than the "true" angle. To derive a measure of the variability in angle judgments produced by such biases, we calculated the resulting angles for 100 sample movies (employing the same parameter randomizations used in the experiments), for each type of motion and various blank periods, and extracted the means and the standard deviations for each condition. Given the balanced nature of our stimulus set we expected, and obtained, means close to the reference angle for all conditions. The standard deviations for each condition can be used to predict the variability in judgments that the biases produce. We calculated angle discriminability as a function of blank period under the assumption that the wider the spread of angles (the larger the standard deviation), the poorer the performance. The dashed lines show the predictions. To account for differences in performance across different motion conditions, the prediction lines were anchored at the respective performance for the "zero blank" conditions.

Discussion

In this paper we have investigated the effect of movement on the discriminability of geometric angles. Rather than considering cases of non-rigid motion, and the resultant shape deformations, which often occur when real objects move (e.g., Loffler & Wilson, 2001), we concentrated on angles that moved rigidly in the fronto-parallel plane. Under these conditions, observers can discriminate angles equally well whether they are static or moving and performance only starts to drop for very fast speeds. The limiting speed is fast enough to impair the visibility of the stimulus and, therefore, at least some of this deterioration can be explained by the spatio-temporal limits of the visual system. Further experiments show performance to be robust in the face of additional background "noise" dots and short periods of occlusion. The degree of robustness is, however, dependent on the motion type, with rotation and expansion being more fragile than translation.

One possibility to explain differences between performance for translation, expansion, and rotation lies within the nature and relationship of the vertex dots' trajectories. Individual dots move in very different ways for different

motion types. In the case of translation, all dots move on linear trajectories with the same constant speed and direction. In the case of expansion, while each individual dot moves on a linear trajectory with constant speed and direction, dots neither share the same speed nor direction. In the case of rotation, dots also differ with respect to both speed and direction but, in addition, move on curved trajectories so that their direction is not constant but changing over time.

These differences in dot trajectories can be linked to the computational complexity faced by the visual system when computing the shape of the dynamic triangles used in this study. For translation, calculating the speed of only one dot is sufficient to compute the overall motion of the stimulus. Hence, the velocity of the apex dot could be used to determine the future position of the other two dots. For expansion, to compute the center of expansion and, therefore, the overall stimulus motion, it is necessary to encode the linear motion of two dots. For rotation, in order to derive the center of rotation and the overall stimulus motion, it is necessary either to encode the circular motion of two dots or to compute the motion of one dot at two different instants. One could, therefore, explain some of our results, most obviously those requiring the extrapolation of the future dot position (Figure 7B), on the basis of differences in the computational complexity of the stimuli.

We next consider how a biologically plausible model can be implemented to account for our main findings. Firstly, what kind of mechanism can explain why angle discrimination is not impaired when triangles are moving? As mentioned previously, a possible candidate is one that relies on the *position* of the three dots and is indifferent to their motion (Figure 8A). A physiologically plausible way of achieving this would be to consider the activation of cells within a retinotopic map, for example the activation of simple cells in V1 (Hubel & Wiesel, 1962). Such cells respond to the triangle dots whether they are static or moving, so the same performance should result for static and any kind of dynamic condition. This mechanism would, however, predict that dynamic angles could not be discriminated when static background dots are added, contrary to the results shown in Figure 6C. Dynamic angle discrimination remains good even if the background dots generate transient signals (by replacing them every frame). This implies that a single mechanism, based on directionally non-specific channels, is insufficient to explain dynamic angle discrimination.

The observation that dynamic performance starts to deteriorate when moving background dots generate a directional signal (i.e., for lifetimes of 2 and more frames; Figure 6C) points toward the involvement of motion-direction-selective channels. A candidate mechanism is one that again integrates information across a retinotopic map, but relies on the activation of motion-direction-selective cells (Figure 8C; Hubel & Wiesel, 1968). As long as the integration stage does not differentiate between absolute directions of motion of the dots, it would respond equally well to translation, rotation, and expansion. This notion cannot, however, explain why we see a different behavior for different types of motions when varying the lifetime of background dots (Figure 6C). Consequently, we have to consider different mechanisms for different motion types (Figures 8D, 8E, and 8F). This is consistent with earlier theoretical and empirical evidence in favor of distinct mechanisms for translational, rotational, and expanding motions. It has been shown that in monkey visual cortex there are neurons selective for translation both in V1 (Hubel & Wiesel, 1968) and MT (Albright, 1984; Movshon & Newsome, 1996). There is also physiological evidence to support the existence of neurons in the medial superior temporal area (MST) that are selective for rotation and expansion/contraction (Duffy & Wurtz, 1991; Tanaka & Saito, 1989). In addition to these physiological studies, psychophysical evidence has been presented to support the existence of distinct mechanisms in the human visual system specialized for rotation (Morrone et al., 1995) and expanding or contracting motion (Burr et al., 1998; Regan & Beverley, 1978).

If computing the *shape* of moving objects was the main objective, why would a system do anything but take "snapshots"? In other words, what are the advantages for employing different computations, depending on the type of motion? One advantage of specific mechanisms is that they can be more resistant against the influence of noise or occlusion than a uniform computation. The fact that performance is unaffected by short "blank periods" (of up to 60 ms) suggests that the actual position of the dots during occlusion is available rather than the location of the dot before it disappeared (see Figure 7B). This can only be achieved using accurate extrapolation. The visual system appears to be able to use the motion signal generated by one vertex dot before the blank period to predict the position of that dot after the blank, when it can be combined with the position and/or motion of the second vertex dot. Given that the same robustness against occlusion is seen for translation, expansion, and rotation, and given that the dots in these conditions move on very different trajectories, this again suggests that distinct computations underlie the three types of motion.

To quantify the efficacy of extrapolation, we calculated performance in the absence of extrapolation, i.e., if the visual system based its calculation of angular magnitude on the position of one of the dots before it disappeared and the position of the other dot when it appeared. This calculation, therefore, integrates positional information across the duration of the blank period but does not extrapolate a dot's position during occlusion based on its motion. The dashed lines in Figure 7C show predictions for the static and the three dynamic conditions (see figure legend for more details). The predictions for the dynamic conditions fail to account for short blanks, where performance remains unaffected (data curves are flat), which requires the visual system to have access to

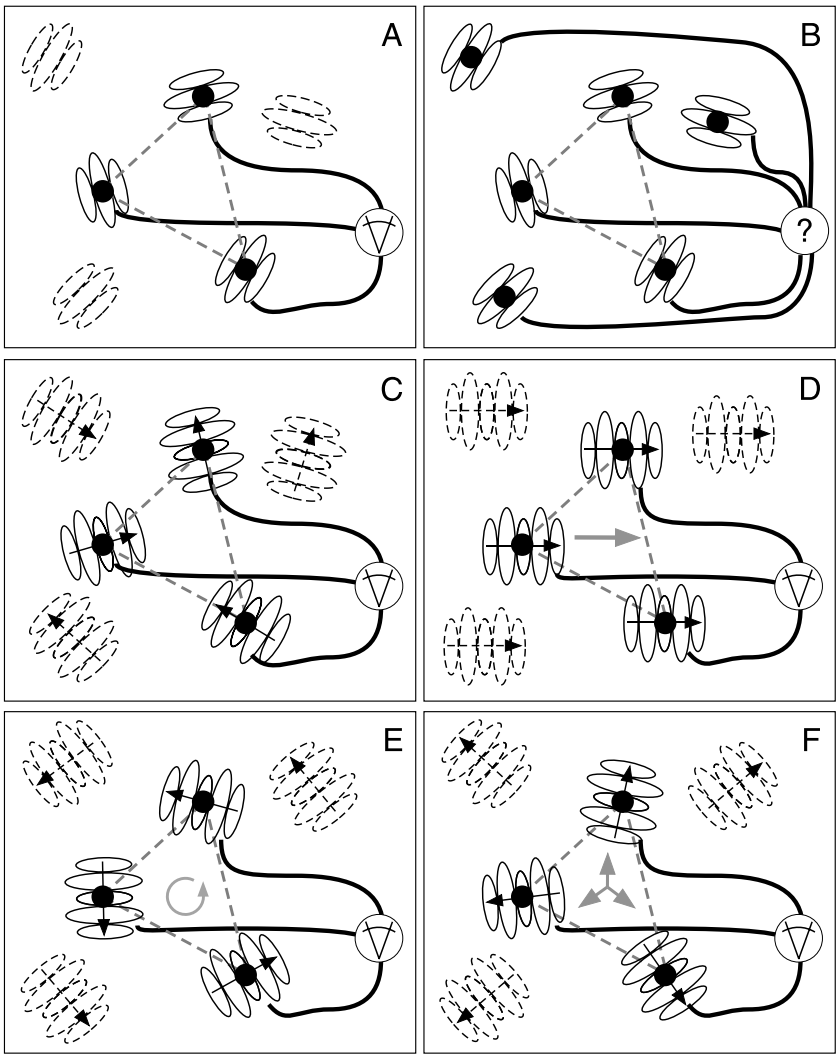

Figure 8. Hypothetical mechanisms for angle measurements in static and dynamic conditions. All models (A–F) are assumed to consist of a two-stage process. At the first stage, the locations of the three dots (black circles) that define the triangle (dashed lines) are encoded by the activation of detectors (receptive fields symbolized by flanked ellipses) within a retinotopic map. Note that in all plots, only a small fraction of detectors are shown for clarity. In all diagrams, active detectors are outlined while inactive detectors are dashed. As indicated by calliper icons, the second stage computes the angular magnitude on the basis of the spatial relationship between first stage detectors' receptive fields. The mechanisms differ with respect to the first stage detectors from which the second stage receives its input, but if one assumes that the same trigonometric computation takes place at the second stage, then the precision with which these mechanisms encode angular magnitude depends on the precision with which the activated first stage detectors can be localized. (A) First stage detectors are orientation-selective cells (e.g., simple cells in V1). Cells with receptive fields centered at the location of each triangle dot are activated and their signals utilized by the second stage. This mechanism would respond in the same way to static or any type of dynamic triangles. Therefore, the mechanism makes the same prediction regardless of the dynamics of the stimulus. (B) Effect of adding background dots to the display. Background dots activate additional first stage detectors, rendering the dots that define the triangle invisible to the second stage process. The temporal duration over which the second stage process sums information can be estimated by altering the lifetime of the background dots. (C) First stage detectors are direction-selective cells (e.g., complex cells in V1, symbolized by a pair of spatially shifted simple-cell receptive fields). The arrows indicate cells' preferred direction of motion. Note that in this model all directions are summed at each location (not shown for clarity), so that any moving stimulus would evoke a response at the relevant location. Hence, this mechanism would make the same prediction for different types of triangle motions (translation, expansion, or rotation) but would not respond to static triangles. (D) In this version, first stage detectors are direction-selective cells, as in "C," but the second stage sums information only from detectors tuned to the same direction of motion (e.g., rightward). This mechanism would respond well to translating motions but not to rotation or expansion. (E) Mechanism analogous to "D" but with a second stage that is tuned for rotation (e.g., counter-clockwise). (F) Mechanism analogous to "D" but with a second stage that is tuned for expansion.

precise positional extrapolation. For longer blank periods, the calculation correctly predicts that the rate at which performance drops is dependent on the type of motion. The slopes of the predictions are higher for rotation versus expansion and translation. Thus, the drop in performance with longer blanks can, at least in part, be explained by a lack of extrapolation and the different nature of the trajectories for the three types of motion. In this scenario, the visual system is biased toward the position of the dot before it disappears and fails to accurately update its current position during occlusion. However, it must be stressed that for short occlusion periods, the visual system must have access to different, but equally accurate, extrapolations for different types of motion, given that individual dots move in different ways depending on the triangle motion.

In summary, the visual system is able to compute angles with the same high precision whether they are moving or not. It appears to do this, not by relying on "snapshots," but rather by employing distinct mechanisms, which are tailored toward the specific kind of motion. This approach allows the visual system to extract moving shapes from a scene even in the presence of background noise and to perform well in situations where parts of the moving shape are occluded for short periods.

Acknowledgments

Part of this work was supported by EPSRC grant # GR/S59239/01 to G.L.

Commercial relationships: none.
Corresponding author: G. Kennedy.
Email: graeme.kennedy@gcal.ac.uk.
Address: Department of Vision Sciences, Glasgow Caledonian University, Cowcaddens Road, Glasgow, G4 0BA, United Kingdom.

References

Albright, T. D. (1984). Direction and orientation selectivity of neurons in visual area MT of the macaque. *Journal of Neurophysiology, 52,* 1106–1130. [PubMed]

Bouma, H., & Andriessen, J. J. (1968). Perceived orientation of isolated line segments. *Vision Research, 8,* 493–507. [PubMed]

Burr, D. C., Morrone, M. C., & Vaina, L. M. (1998). Large receptive fields for optic flow detection in humans. *Vision Research, 38,* 1731–1743. [PubMed]

Chen, S., & Levi, D. M. (1996). Angle judgment: Is the whole the sum of its parts? *Vision Research, 36,* 1721–1735. [PubMed]

Chen, S., & Levi, D. M. (1997). Angle discrimination and orientation discrimination in central and peripheral vision (Abstract). *Investigative Ophthalmology and Visual Science, 38,* S631.

Coppola, D. M., Purves, H. R., McCoy, A. N., & Purves, D. (1998). The distribution of oriented contours in the real world. *Proceedings of the National Academy of Sciences of the United States of America, 95,* 4002–4006. [PubMed] [Article]

De Bruyn, B., & Orban, G. A. (1988). Human velocity and direction discrimination measured with random dot patterns. *Vision Research, 28,* 1323–1335. [PubMed]

Duffy, C. J., & Wurtz, R. H. (1991). Sensitivity of MST neurons to optic flow stimuli. I. A continuum of response selectivity to large-field stimuli. *Journal of Neurophysiology, 65,* 1329–1345. [PubMed]

Elder, J. H., & Goldberg, R. M. (2002). Ecological statistics of Gestalt laws for the perceptual organization of contours. *Journal of Vision, 2*(4):5, 324–353, http://journalofvision.org/2/4/5/, doi:10.1167/2.4.5. [PubMed] [Article]

Farah, M. J., Wilson, K. D., Drain, M., & Tanaka, J. N. (1998). What is "special" about face perception? *Psychological Review, 105,* 482–498. [PubMed]

Field, D. J., Hayes, A., & Hess, R. F. (1993). Contour integration by the human visual system: Evidence for a local "association field." *Vision Research, 33,* 173–193. [PubMed]

Geisler, W. S., Perry, J. S., Super, B. J., & Gallogly, D. P. (2001). Edge co-occurrence in natural images predicts contour grouping performance. *Vision Research, 41,* 711–724. [PubMed]

Heeley, D. W., & Buchanan-Smith, H. M. (1996). Mechanisms specialized for the perception of image geometry. *Vision Research, 36,* 3607–3627. [PubMed]

Hubel, D. H., & Wiesel, T. N. (1962). Receptive fields, binocular interaction and functional architecture in the cat's visual cortex. *The Journal of Physiology, 160,* 106–154. [PubMed] [Article]

Hubel, D. H., & Wiesel, T. N. (1968). Receptive fields and functional architecture of monkey striate cortex. *The Journal of Physiology, 195,* 215–243. [PubMed] [Article]

Kelly, D. H. (1979). Motion and vision. II. Stabilized spatio-temporal threshold surface. *Journal of the Optical Society of America, 69,* 1340–1349. [PubMed]

Kennedy, G. J., Orbach, H. S., & Loffler, G. (2006). Effects of global shape on angle discrimination. *Vision Research, 46,* 1530–1539. [PubMed]

Koenderink, J. J. (1986). Optic flow. *Vision Research, 26,* 161–179. [PubMed]

Loffler, G., & Wilson, H. R. (2001). Detecting shape deformation of moving patterns. *Vision Research, 41,* 991–1006. [PubMed]

McKee, S. P., Silverman, G. H., & Nakayama, K. (1986). Precise velocity discrimination despite random variations in temporal frequency and contrast. *Vision Research, 26,* 609–619. [PubMed]

Morrone, M. C., Burr, D. C., & Vaina, L. M. (1995). Two stages of visual processing for radial and circular motion. *Nature, 376,* 507–509. [PubMed]

Movshon, J. A., & Newsome, W. T. (1996). Visual response properties of striate cortical neurons projecting to area MT in macaque monkeys. *Journal of Neuroscience, 16,* 7733–7741. [PubMed] [Article]

Nakayama, K. (1981). Differential motion hyperacuity under conditions of common image motion. *Vision Research, 21,* 1475–1482. [PubMed]

Orban, G. A., Vandenbussche, E., & Vogels, R. (1984). Human orientation discrimination tested with long stimuli. *Vision Research, 24,* 121–128. [PubMed]

Pelli, D. G. (1997). The VideoToolbox software for visual psychophysics: Transforming numbers into movies. *Spatial Vision, 10,* 437–442. [PubMed]

Quick, R. F., Jr. (1974). A vector-magnitude model of contrast detection. *Kybernetik, 16,* 65–67. [PubMed]

Regan, D., & Beverley, K. I. (1978). Looming detectors in the human visual pathway. *Vision Research, 18,* 415–421. [PubMed]

Regan, D., Gray, R., & Hamstra, S. J. (1996). Evidence for a neural mechanism that encodes angles. *Vision Research, 36,* 323–330. [PubMed]

Robson, J. G. (1966). Spatial and temporal contrast-sensitivity functions of the visual system. *Journal of the Optical Society of America, 56,* 1141–1142.

Scobey, R. P. (1982). Human visual orientation discrimination. *Journal of Neurophysiology, 48,* 18–26. [PubMed]

Snippe, H. P., & Koenderink, J. J. (1994). Discrimination of geometric angle in the fronto-parallel plane. *Spatial Vision, 8,* 309–328. [PubMed]

Stone, L. S., & Thompson, P. (1992). Human speed perception is contrast dependent. *Vision Research, 32,* 1535–1549. [PubMed]

Tanaka, K., & Saito, H. (1989). Analysis of motion of the visual field by direction, expansion/contraction, and rotation cells clustered in the dorsal part of the medial superior temporal area of the macaque monkey. *Journal of Neurophysiology, 62,* 626–641. [PubMed]

Thompson, P. (1982). Perceived rate of movement depends on contrast. *Vision Research, 22,* 377–380. [PubMed]

Valentine, T. (1991). A unified account of the effects of distinctiveness, inversion, and race in face recognition. *Quarterly Journal of Experimental Psychology A: Human Experimental Psychology, 43,* 161–204. [PubMed]

Watamaniuk, S. N., Sekuler, R., & Williams, D. W. (1989). Direction perception in complex dynamic displays: The integration of direction information. *Vision Research, 29,* 47–59. [PubMed]

Werkhoven, P., & Koenderink, J. J. (1993). Visual size invariance does not apply to geometric angle and speed of rotation. *Perception, 22,* 177–184. [PubMed]

Wilkinson, F., Wilson, H. R., & Habak, C. (1998). Detection and recognition of radial frequency patterns. *Vision Research, 38,* 3555–3568. [PubMed]